SAND99-0308C

Fabrication, Packaging, and Performance of VCSELs and Photodetectors for Space Applications

R. D. Briggs, M. G. Armendariz, K. M. Geib, K. D. Choquette and D. K. Serkland

Sandia National Laboratories, Albuquerque, NM 87185-0603

ABSTRACT

Optocouplers are used for a variety of applications aboard spacecraft including electrical isolation, switching and power transfer. Commercially available light emitting diode (LED)-based optocouplers have experienced severe degradation of light output due to extensive displacement damage occurring in the semiconductor lattice caused by energetic proton bombardment. A new optocoupler has been designed and fabricated which utilizes vertical cavity surface emitting laser (VCSEL) and resonant cavity photodetector (RCPD) technologies for the optocoupler emitter and detector, respectively. Linear arrays of selectively oxidized GaAs/AlGaAs VCSELs and RCPDs, each designed to operate at a wavelength of 850nm, were fabricated using an airbridge contacting scheme. The airbridged contacts were designed to improve packaging yields and device reliability by eliminating the use of a polyimide planarizing layer which provided poor adhesion to the bond pad metallization. Details of the airbridged optocoupler fabrication process are reported. Discrete VCSEL and RCPD devices were characterized at temperatures between -100° C to 100° C. Devices were packaged in a face-to-face configuration to form a single channel optocoupler and its performance was evaluated under conditions of high-energy proton bombardment.

Keywords: Vertical cavity surface emitting lasers (VCSELs), resonant cavity photodetectors (RCPDs), optocouplers, space, radiation, proton.

INTRODUCTION

Optocouplers are used on spacecraft flight modules for a variety of applications such as electrical isolation, switching, and power transfer and typically consist of an LED transmitter coupled with a p-i-n photodiode or phototransistor. Because of their widespread use, it is not always possible or desirable to provide the optocouplers with the necessary shielding for protection from radiation exposure. Recent NASA missions by the TOPEX spacecraft and the Hubble Space Telescope have experienced radiation induced failures of the on-board commercial LED optocouplers due to damage in the semiconductor lattice resulting from collisions with energetic protons[1,2]. These devices were susceptible to radiation-induced failure at equivalent total dose levels of 10 to 20 krad(Si) with severe degradation of light output occurring at 1 to 3 krad(Si). The X2000 program at Jet Propulsion Laboratories is currently developing advanced flight instrumentation for a series of NASA missions with extreme radiation requirements. A planned mission to the Europa moon of Jupiter is particularly challenging because the total radiation dose levels may exceed 1 Mrad(Si). Several important considerations must be considered when choosing devices for space applications including reliability, lifetime, power consumption, size, temperature response, and radiation tolerance. VCSELs have been the subject of widespread research and development for the past decade and are now entering the marketplace in products for optical data communications[3]. Both VCSELs and RCPDs, which may be fabricated monolithically utilizing the same semiconductor epitaxy, exhibit great promise for use in space environments[4,5]. Sandia National Laboratories is collaborating with Jet Propulsion Laboratories to develop radiation hardened VCSEL- and RCPD-based optocouplers which may be broadly applicable to a variety of NASA missions, including the Jupiter mission set. The target specifications for these devices are listed in Table 1.

Optocoupler Specification	
Radiation Hardness	> 1Mrad
Operating Temperatures	-80°C to 70°C
Power Consumption	< 5 mW/channel
Power Supply Voltage	3.3 V
Size	~ 1cm^3 (16 channels)

Table 1. Device requirements for JPL optocouplers.

DISCLAIMER

The epitaxial structure of VCSELs and RCPDs consists of two high-reflectivity distributed Bragg reflector (DBR) mirrors separated by an optical cavity typically 1-λ thick (where λ is the wavelength of light in the semiconductor) to form a high finesse Fabry-Perot cavity. The DBR mirrors provide longitudinal confinement of light within the laser and are composed of repeating pairs of quarter-wavelength thick high and low refractive index monolithically grown semiconductor layers. The optical cavity contains the laser active region, usually consisting of 1 to 5 quantum wells. Providing electrical contacts to the p- and n-type DBR mirrors forms the laser diode. Air-posts, ion implantation, and selective oxidation are all means of providing the transverse optical and electrical confinement necessary to define the lateral extent of the laser cavity. Air-posts have the advantages of simple fabrication and index-guided optical confinement but suffer from high optical loss and poor thermal dissipation. Ion implanted VCSELs offer the advantages of planar geometry, enhanced heat sinking, and defined current confinement, however, they lack intrinsic optical confinement which limits their threshold and modulation characteristics. Selectively oxidized VCSELs utilize buried AlGaAs layers to effectively define the transverse laser cavity[6]. The incorporation of electrically insulating low refractive index oxide layers within the VCSEL provides efficient current injection and index-guided optical confinement resulting in reduced series resistance, lower threshold currents, and higher efficiencies. Selectively oxidized VCSELs require the etching of mesas to expose the buried AlGaAs layers for oxidation. Typically, a polyimide film is deposited to planarize the surface prior to packaging, however, this process suffers from very low packaging yields due to poor bond pad adhesion to the polyimide. Studies have shown that the deposition of a TiAu bond pad directly upon a Si_3N_4 dielectric film or the semi-insulating substrate provides the greatest bond yields and adhesion strengths[7]. Bond pull tests performed on polyimide planarized test structures resulted in zero yield due delamination of contacts before measurement was possible. TiAu contacts consisting of 500nm Ti and 0.07 to 5.0 μm fo Au deposited on 200 nm Si_3N_4 had average bond strengths of 7.23 gm and a packaging yield of 100% on 480 bonds. A robust manufacturing process was developed utilizing airbridged interconnects to contact the top DBR mirror ohmic metals to bond pads located on the lower DBR plane, thus eliminating the use of polyimide and incorporating the TiAu on Si_3N_4 structure. This new process increased packaging yields dramatically due to the improved bond pad adhesion.

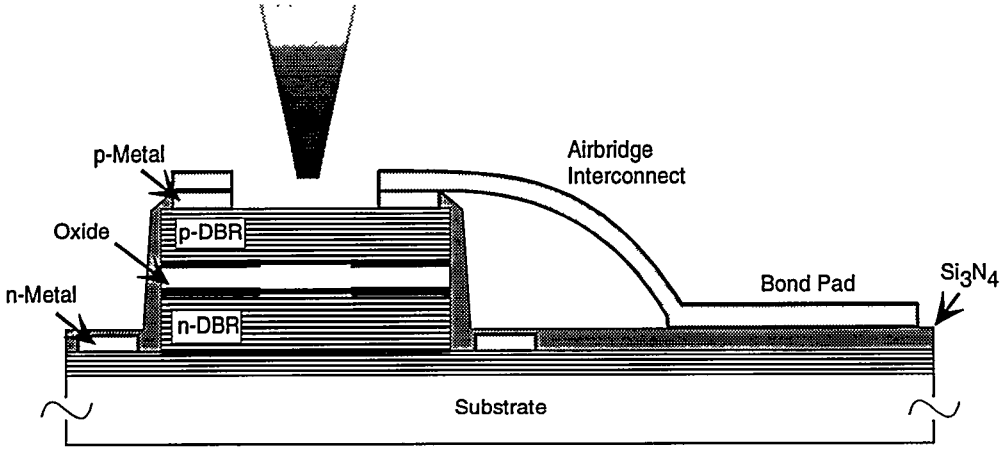

Figure 1. Cross section sketch of a selectively oxidized VCSEL with an airbridge. The airbridge connects the top DBR p-type ohmic contact to the bond pad and spans the n-type ohmic contact ring at the base of the mesa.

DEVICE FABRICATION

Selectively oxidized VCSELs were fabricated using a mesa structure to allow for oxidation and airbridges to create coplanar bond pads as seen in Figure 1. The epitaxial structure was grown in a rotating-disc metal organic vapor phase epitaxy (MOVPE) reactor with *in-situ* diagnostics designed to maintain accurate doping, layer composition, and layer thicknesses. For devices designed to operate at a wavelength of 850 nm, the lower DBR consisted of 36 periods of a n-doped unit structure consisting of a low refractive index $Al_{0.92}Ga_{0.08}As$ layer and a high index $Al_{0.16}Ga_{0.84}As$ layer with an intermediate layer containing linearly graded Al composition. The active region contained 5 GaAs quantum wells separated by $Al_{0.20}Ga_{0.80}As$ barriers and the top mirror structure had 21 periods of p-doped material similar to the bottom DBR. In one

period on each side of the active region a single layer of $Al_{0.98}Ga_{0.02}As$ was substituted for the low index layer and will be used to form the buried oxide aperture. For the purpose of the demonstration, RCPDs were fabricated from a second wafer which was grown with an identical epitaxial structure with the exception that the top DBR only contains 10 mirror pairs. The fabrication process for the two devices was also identical with the exception that the RCPDs did not require oxidation. Monolithic integration of the devices has also been demonstrated by using a buried ¾λ etch stop layer within the top DBR structure and then removing the top DBR pairs from the RCPDs with a reactive ion etch (RIE)[8,9].

Fabrication begins with the lift-off deposition of TiPtAu (20/20/200 nm) p-type ohmic contacts to the top DBR structure. A BCl_3-based inductively coupled plasma etch is used to pattern square mesas and expose the sidewalls for oxidation followed by lift-off deposition of GeAuNiAu (26/54/15/200 nm) n-type ohmic contacts to the lower DBR. A laser beam reflectance monitor is used during the etch to stop precisely on one of the high index $Al_{0.16}Ga_{0.84}As$ layers within the lower DBR. This results in lower contact resistances than those measured in contacts made to the low index $Al_{0.92}Ga_{0.08}As$ material due to its tendency to oxidize during device processing. Wet oxidation of the buried $Al_{0.98}Ga_{0.02}As$ layers is performed in a three-zone furnace fitted with a water bubbler at 440° C for ~15 minutes. Process control monitors included in the dicing streets of the mask design incorporate calibration mesas which allow for targeting oxidation apertures to 1 μm accuracy. A 200 nm thick PECVD Si_3N_4 inter-level dielectric film is deposited to encapsulate the sidewalls of the device and passivate the surface of the exposed lower DBR to provide a region for bond pad formation. A RIE etch is used to pattern the Si_3N_4 to provide contact holes to the n- and p-type ohmic contacts. A 5 μm thick sacrificial layer of PMGI SF-19 is deposited, patterned and reflowed to provide support for the airbridge metallization. PMGI is particularly useful because it is photodefinable with deep utraviolet (DUV) light and impervious to acetone, therefore allowing it to remain in place for the remainder of the fabrication process. It provides mechanical support for the airbridges and protects the semiconductor surface of the VCSEL aperture. A thin TiAu (5/50 nm) seed layer is deposited over the PMGI and then 2μm of Au is electroplated to form the airbridges and bond pads. The TiAu seed layer is sputtered away using an Ar reactive ion beam etch (RIBE) and the fabrication is completed with the removal of the PMGI layer by soaking in a heated solution of N-methylpyrrolidone. Scanning electron micrographs (SEM) of the completed devices are shown in figure 2. Arrays of VCSELs and RCPDs were then separated using a dicing saw and packaged in 24 pin DIP packages.

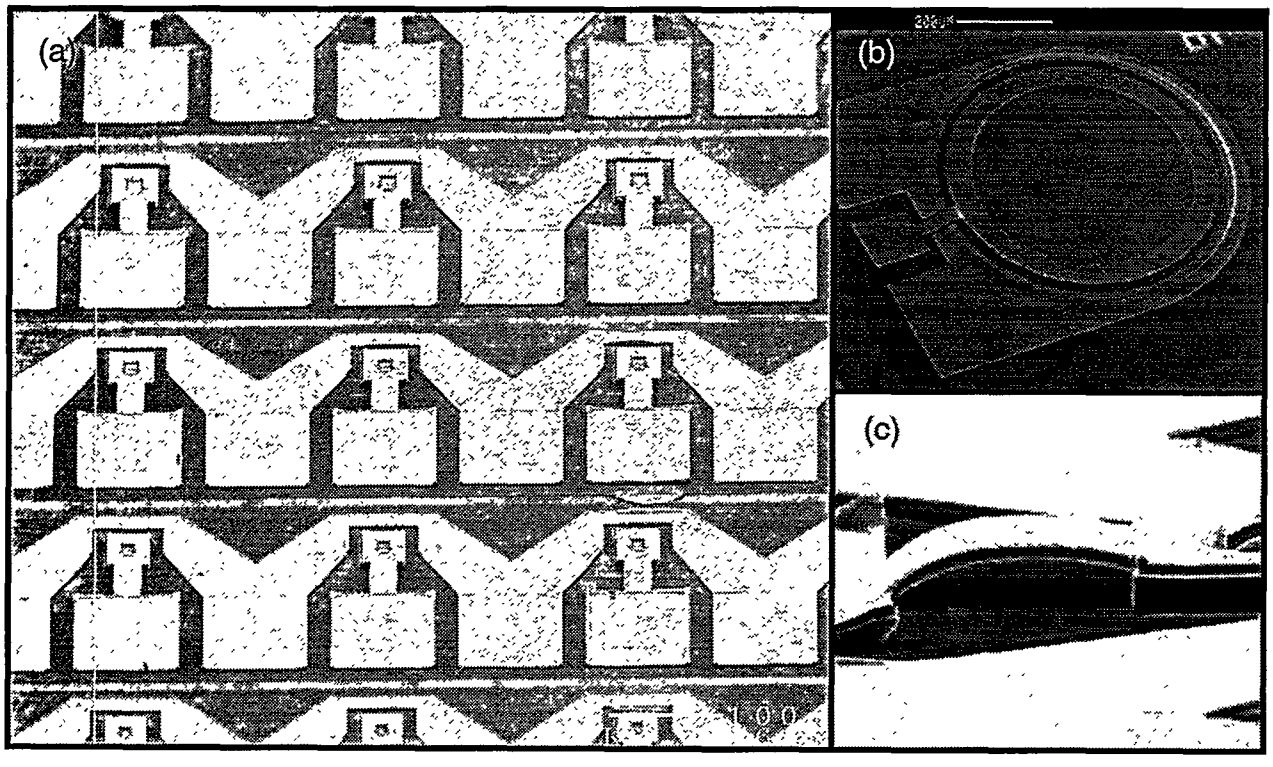

Figure 2. (a) Linear arrays of selectively oxidized VCSELs, aperture sizes of 3x3 μm, 5x5 μm, and 7x7 μm, with coplanar airbridged contacts. *(b)* Airbridged large area RCPD. *(c)* Side view close-up of 2.0 μm thick airbridge formed from electroplated Au.

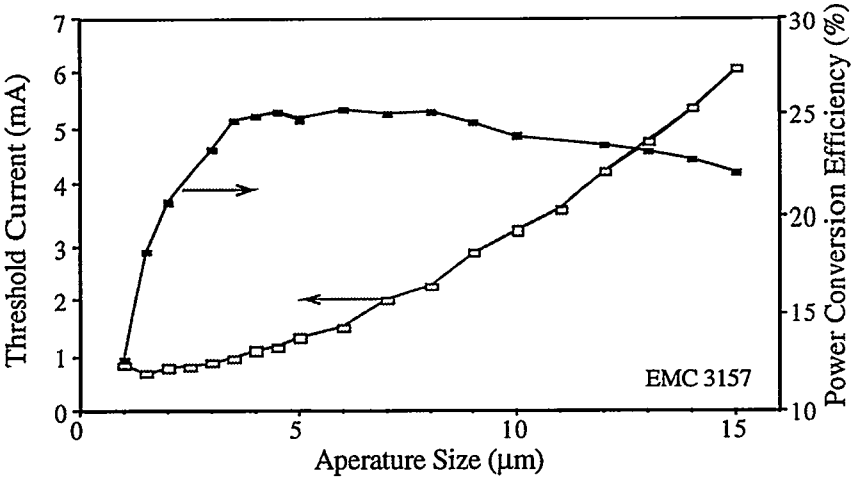

Figure 3. Threshold current and maximum power conversion efficiency of selectively oxidized VCSELs.

DEVICE CHARACTERIZATION

In Figure 3 the threshold current and maximum power conversion efficiency is plotted as a function of oxide aperture size. Notice that the highest conversion efficiencies with the lowest threshold currents occur for 5x5 μm devices, which are the focus of the following device characterization. Representative light and voltage versus current (LIV) and power conversion efficiency curves for a 5x5 μm device measured at room temperature are shown in Figure 4. The threshold current is

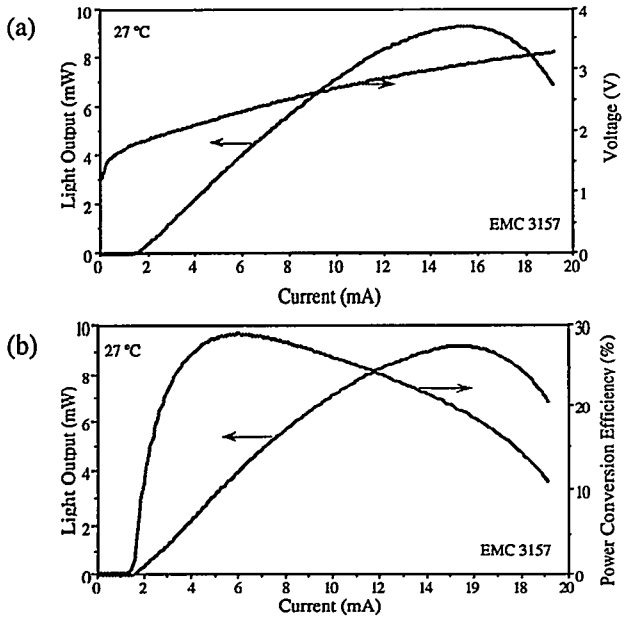

Figure 4. *(a)* LIV and *(b)* power conversion efficiency of 5x5 μm selectively oxidized VCSELs.

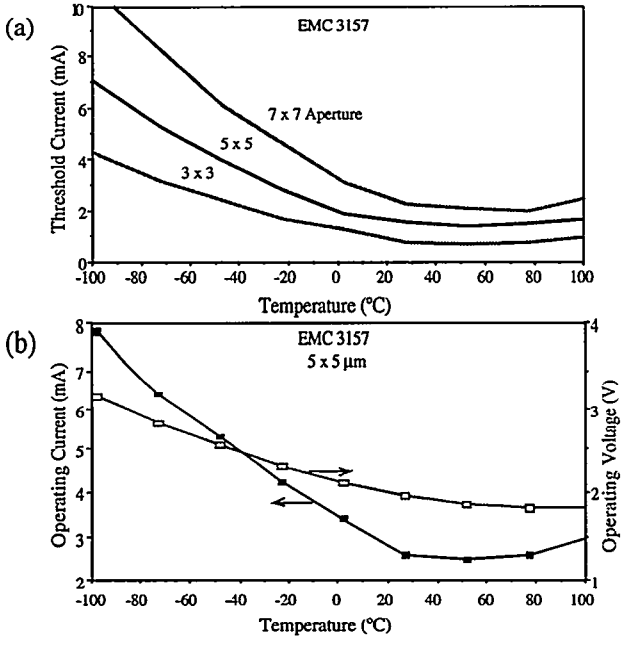

Figure 5. Temperature characteristics of 5x5 μm selectively oxidized VCSELs: *(a)* threshold current and *(b)* operating current and voltage to produce 1 mW output power.

approximately 1.85 mA and the threshold voltage is 1.75 V. Maximum light output power of 9.4 mW is achieved with an input current of 15 mA and the maximum efficiency of 28% occurs at approximately 5 mW output power for this VCSEL. The operating characteristics of the VCSELs over a temperature range from –100° C to 100° C is shown in Figure 5. The threshold current in figure 5(a) reaches a minimum value at a temperature (~50° C for the 5x5 μm device) where the cavity resonance spectrally matches the laser gain bandwidth. The cavity resonance is determined primarily by the DBR layer thickness and refractive index while the laser gain is determined by the quantum well thickness. Both the laser gain and cavity resonance shift to longer wavelengths with increasing temperature, however, the gain curve shifts at a faster rate. To compensate for this phenomenon, VCSELs are designed with an intentional spectral blue shift of the laser gain relative to the cavity resonance. In order to optimize the VCSELs for space applications, the cavity resonance must be redesigned to reduce the amount of spectral compensation for device heating. This should result in the threshold current curves that are more symmetric with respect to the desired temperature range and therefore lower threshold currents would be required for low temperature operation. As seen in Figure 5(b), the operating voltage required to maintain 1 mW output power in the 5x5 μm VCSEL remains less than the 3.3V specification for the entire temperature range. However, the operating current soars to >8 mA at the lowest temperatures of interest.

The spectral responsivity of a RCPD is shown in Figure 6. The cavity resonance and hence peak responsivity shift to longer wavelengths with increasing temperature although the FWHM spectral bandwidth remains fairly constant at approximately 10 nm. The increase in center wavelength is a result of the same cavity temperature effect observed in the VCSELs and occurs primarily due to the temperature dependence of the refractive index in the layers of the DBR. The increased responsivity is similarly related to the overlap of the cavity resonance with the spectral bandwidth of the absorption region. This is more clearly seen in Figure 6(b) where the peak responsivity is plotted as a function of ambient temperature. Below -100° C the excitonic absorption has shifted away from the cavity resonance such that the absorption of photons is decreased. The peak occurring at approximately -50° C is related to the excitonic absorption peak below the band edge. As the temperature continues to increase the band gap becomes smaller resulting in increased photon absorption and increased peak responsivity at the cavity resonance. It should be noted that one advantage of monolithic VCSEL/RCPD optocouplers is that the laser and detector peak wavelengths will shift coincidentally with ambient temperature changes.

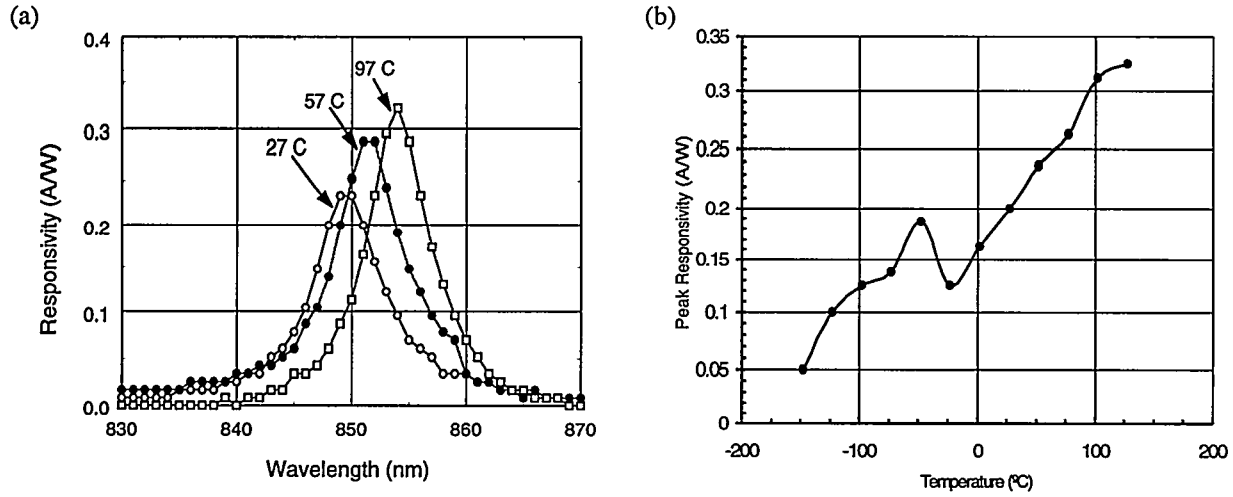

Figure 6. *(a)* Spectral responsivity of a RCPD using a reverse bias of –3V and *(b)* the peak responsivity as a function of ambient temperature.

RADIATION CHARACTERIZATION

Optocouplers on a spacecraft can experience high fluence levels of energetic protons and electrons causing significant radiation-induced damage. Protons can produce both ionizing irradiation damage and lattice displacement damage while electrons produce primarily ionizing radiation damage. In VCSELs, the displacement of lattice atoms through collision with energetic protons causes the creation of defects that act as efficient non-radiative recombination centers and results in

degradation of light output. The effects of irradiation on optocouplers were characterized at the Indian University Cyclotron Facility by irradiating components with protons at energies of 52 to 192 MeV to fluences from $5x10^{11}$ to $3X10^{14}$ protons/cm^2. The data taken at multiple energy levels can be used to calculate more precise estimates of device degradation for the proton spectrum in the actual space environment, however, only the highest energy data will be summarized in this discussion. For this project, the radiation tolerance specification is less than 40% degradation at a total dose of 1 Mrad(Si) which corresponds to a proton fluence of $1.66x10^{13}$ protons/cm^2 at an energy level of 192 MeV. Figure 7 is a plot of the optocoupler output photocurrent measured at a reverse bias of –3.3V versus laser input current. For fluence levels below $2x10^{13}$ protons/cm^2 (1.2 Mrad(Si)), there is virtually no effect on the optocoupler output. At a fluence of $5x10^{13}$ protons/cm^2 (>3 Mrad(Si)), the threshold current increases by ~0.5mA and the peak photocurrent drops ~5 μA. The optocoupler normalized output photocurrent as a function of increasing proton fluence is shown in Figure 8. Less than 10% device degradation is realized for a total dose of greater than 3 Mrad(Si). These devices display a much higher degree of radiation hardness than the current LED-based optocouplers which typically experienced ~50% degradation at fluence levels as low as $3x10^{11}$ protons/cm^2.

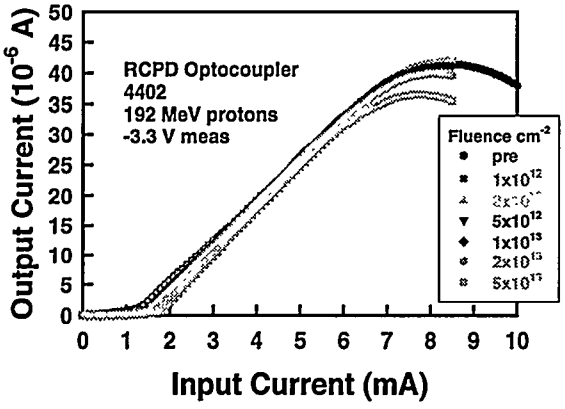

Figure 7. RCPD output photocurrent versus VCSEL input current for increasing levels of proton irradiation.

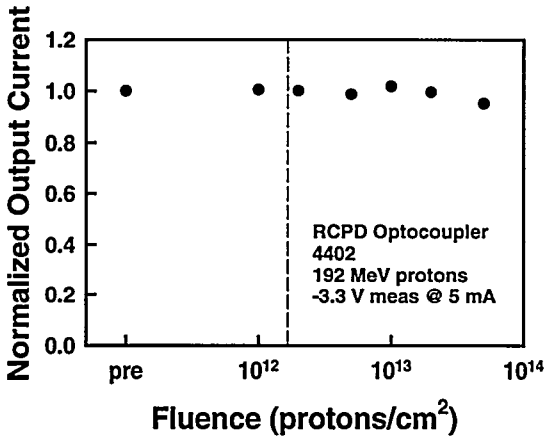

Figure 8. Normalized RCPD/VCSEL optocoupler output photocurrent (measured at a reverse output bias of –3.3V and an input current of 5 mA) versus fluence.

CONCLUSION

An airbridge fabrication process has been developed for manufacturing mesa isolated selectively oxidized VCSELs and RCPDs for use in space applications. Typically, mesa isolated optoelectronic devices are planarized using a thick polyimide dielectric film. In this process, bond pads are deposited on a thin Si_3N_4 film or directly on the semi-insulating GaAs substates and airbridged interconnects are used to make contact the top DBR structures of the optoelectronic devices. The resulting increase in bond pad adhesion strength improved packaging yields dramatically. Linear arrays of VCSELs and RCPDs were fabricated and tested for temperature stability over a range from –100° C to 100° C. Although characterized devices met the required project specifications, some optimization in the design of the DBR mirror stacks is required to enhance low temperature operation. A single channel optocoupler was packaged and tested for radiation hardness by irradiating the devices with energized protons. The devices experienced less than 10% degradation in output photocurrent for fluence levels equivalent to 3 Mrad(Si). These devices are excellent candidates for replacing current commercially available optocouplers on future space missions to extreme radiation environments.

ACKNOWLEDGEMENTS

This work was supported by the United States Department of Energy under Contract DE-AC04-94AL85000. Sandia is a multiprogram laboratory operated by Sandia Corporation, a Lockheed Martin Company, for the United States Department of Energy.

REFERENCES

1. B.G. Rax, C.I. Lee, A.H. Johnston, C.E. Barnes, "Total dose and proton damage in optocouplers", *IEEE Trans. Nucl. Sci.* **43**, 3167 (1996).
2. K.A. LaBel, P.W. Marshall, C.J. Marshall, M. D'Ordine, M. Carts, G. Lum, H.S. Kim, C.M. Seidleck, T. Powell, R. Abbott, J. Barth, and E.G. Stassinopoulos, "Proton-induced transients in optocouplers: in-flight anomalies, ground irradiation test, mitigation and implications", *IEEE Trans. Nucl. Sci.* **44**, 1885 (1997).
3. K. Choquette and H. Hou, "Vertical cavity surface emitting lasers: moving from research to manufacturing", *Proc. IEEE*, **85**, 1730 (1997).
4. A. Paxton, R. Carson, H. Schone, E. Taylor, K. Choquette, H. Hou, K. Lear and M. Warren, "Damage from proton irradiation of vertical cavity surface emitting lasers", *IEEE Trans. Nucl. Sci.* **44**, 1285 (1997).
5. R. Carson, E. Taylor, A. Paxton, H. Schone, K. Choquette, H. Hou, M. Warren, and K. Lear, "Surface emitting laser technology and its application to the space radiation environment", *SPIE Critical Reviews of Technology*, **CR-62**, 121 (1997).
6. K.D. Choquette, H.Q. Hou, K.M. Geib, B.E. Hammons, "Selectively oxidized vertical cavity laser performance and technology", *Photon. Tech. Lett.*, **7**, 1237 (1995).
7. P.K. Seigal, R.D. Briggs, D.J. Reiger, A.G. Baca, and A.J. Howard, "Adhesion studies of GaAs-based ohmic contact and bond pad metallization", *Thin Solid Films*, **291**, 503 (1996).
8. G.G. Ortiz, C.P. Hains, J. Cheng, H.Q. Hou, and J.C. Zolper, "Monolithic integration of $In_{0.2}Ga_{0.8}As$ vertical-cavity surface-emitting lasers with resonance-enhanced quantum-well photodetectors", *Elect. Lett.*, **32**, 1205 (1996).
9. K.M. Geib, K.D. Choquette, A.A. Allerman, J.J. Hindi, J. Nevers, and B.E. Hammons, "Monolithically integrated VCSELs and photodetectors for microsystem applications", *1998 LEOS Annual Meeting Conference Proceedings*, 27 (1998).